MODELING THE OUTLET TEMPERATURE IN HEAT EXCHANGERS
Case Study

by

Alina BARBULESCU[a] and Lucica BARBES[b*]

[a] Department of Civil Engineering, Transilvania University of Brasov, Brasov, Romania
[b] Department of Chemistry and Chemical Engineering, Ovidius University of Constanta, Constanta, Romania

Original scientific paper
https://doi.org/10.2298/TSCI190913449B

This article presents the results of the study of the heat transfer in a heat exchanger where the working fluid is the crude oil prepared for desalination, and the thermic agent is the re-circulating heavy gasoline fraction. Firstly, the Reynolds numbers have been computed using the temperatures and flow rates of the fluids as input variables. Then, general regression neural network and multilayer perceptron were used for the outlet temperatures estimation using the inlet temperatures and the Reynolds numbers as input variables. The best models on the training dataset were obtained utilizing a multilayer perceptron with one hidden layer, while the best performance on the validation dataset was obtained using a multilayer perceptron network with two hidden layers

Key words: *heat transfer, neural networks, Reynolds number, outlet temperature*

Introduction

Thermal integration techniques have rapidly evolved in parallel with the evolution of industrial analysis and control systems. The apparition of the Pinch technique marked the starting point of the development of energy reduction and conservation techniques. At the beginning, Pinch technique was successfully used in the analysis of simple heat exchangers networks. Due to its improvement, now it is also utilized in complex industrial plants. Through Pinch analysis and mathematical modeling, the necessary quantities of utilities in a process can be reduced and implicitly the total cost of the experimental or industrial installations will decrease [1]. A significant variety of computational algorithms has been developed the same time: Box-Jenkins methods [2, 3], non-linear programming with artificial neural networks (ANN) [4], fuzzy models [5], generalized disjunctive programming, and mixed-integer non-linear programming [6].

To facilitate the design of heat exchangers for improving the energy consumption and reducing the plant total cost, specialized software has been developed. Whether the plant is analyzed by components or as a whole, the thermic integrated processes are more unstable and difficult to control after integration, due to the degrees of freedom reduction. This issue needs to be assessed by identifying viable solutions using control schemes (proportional--integral-derivative or advanced control) that are consistent with the design achieved after in-

* Corresponding author, e-mail: lucille.barbes2009@gmail.com

tegration. In the technological installations of the oil processing plants, the tubular heat exchangers play a major role in the thermal transfer, in processes such as heating, preheating, cooling, condensation, vaporization, *etc.* This category of equipment includes shell-and-tube and tube-in-tube heat exchangers. Heat exchangers shell-and-tube are the most used due to their simple construction, low pressure loss and easy maintenance.

Some studies on heat exchangers concern the design and development of shell-and--tube heat exchangers [7-9], plate type heat exchangers [10], applications of compact heat exchangers [11], an improved threshold fouling model which incorporates the effects of both bulk and surface temperatures [12, 13], and CFD applications in heat exchangers' design [14, 15]. As an alternative to the deterministic approaches [16] for solving the problems related to the heat transfer, some authors chose the ANN [17-21]. Islamoglu [18] used ANN to predict the heat transfer rate of the wire-on-tube type HX, using a back-propagation algorithm for training and testing the network, with very good results (errors between 0% and 8%). Moya-Rico *et al.* [19] presented an ANN model for predicting the heat transfer rate and pressure drop in a triple concentric-tube heat exchanger used in the food industry. The input variables were the helix pitch, groove depth, outer diameter, cold fluid mass-flow rate, cold fluid temperature at the inlet, hot fluid mass-flow rate and hot fluid temperature at the inlet, respectively. The outputs were the heat transfer rate, and the pressure drop. Pacheco-Vega *et al.* [20] applied the ANN to heat exchangers for refrigeration applications with atmospheric air flowing outside and Freon 22 flowing inside. Eleven independent input variables were used and the total heat rate was evaluated by a feed-forward network. Verma *et al.* [21] investigated the energy loss due to the employment of corrugated/non-corrugated pipes as outer/inner shells/tubes in a shell-and-tube heat exchanger utilizing ANN. Eight input parameters have been considered and three output parameters have been estimated (Nusselt and Reynolds numbers, and the overall heat transfer coefficient). Recently, Dheenamma *et al.* [22] developed ANN models for predicting the output plate heat exchanger parameters (overall heat transfer coefficient, effectiveness factor, friction factor of cold and hot fluids), utilizing four (cold and hot fluid Reynolds and Prandtl numbers) or five (concentration of the cold fluid cold and hot fluid Reynolds and Prandtl numbers) input parameters. Mohanraj [23] reviewed some applications of ANN for different heat transfer equipment and found that most architectures of the neural networks for thermal analysis of heat exchangers are multilayer feed forward networks, while only very few are neuro fuzzy interface systems or radial biased function networks.

This article contains the results of the heat transfer study in a heat exchanger where the working fluid is the crude oil prepared for desalination, and the thermic agent is the re-circulating heavy gasoline fraction. The modeling has been performed in two stages. General regression neural networks (GRNN) and multilayer perceptron (MLP) have been utilized for estimating the outlet temperatures, given the values of four input parameters. Different architectures of the networks have been proposed and tested. Comparisons of results are provided. Based on our knowledge there is no article treating comparatively the performances of the estimations of the outlet temperature obtained by MLP and GRNN on the shell-and-tube exchangers of the type presented here.

Methodology

The experimental study is based on the analysis of the heat transfer realized between the re-circulating gasoline (twice in the shell side) and the crude oil that circulate in counter flow in a shell-and-tube heat exchanger which is designed, built and operates at industrial scale. The gasoline is generated in the distillation column of crude oil.

The flow in the heat exchanger considered in this study has an *U*-shaped design with a single pass for the thermal agent and two passes for the working fluid. The experiment took place during the normal operation of an industrial plant that is fully automated and whose working parameters are continuously monitored. The plant was operating in a stationary regime. The change of raw material flow rate is made every few days, depending on the quantities required for delivery. This way, experimental data sets were collected for the chosen type of heat exchanger. The overall technological objective of the heat transfer was to assure a certain temperature of the crude oil at the exchanger outlet, to meet the temperature condition imposed in the subsequent processing steps. The modeling comprises two steps.

Step 1. The input data were the temperature and flow rates of the crude oil (working fluid) and gasoline (thermic fluid) collected as aforementioned, while the output was formed by the Reynolds numbers of both fluids.

To make an energy balance of the two fluids, the following is assumed: no heat loss, negligible potential and kinetic energy changes, no phase changes, constant specific heat capacity, and steady-state conditions.

The heat transfer balance for the stationary process is satisfied by the equality between the two thermic fluxes of hot, Q_h, and cold fluids, Q_c, if the heat loss to the exterior is neglected, meaning that:

$$Q_h = Q_c = Q \tag{1}$$

The heat transfer balance between the tube side and the shell side is given by:

$$Q = \dot{m}_h c_{p,h}(t_{h,i} - t_{h,o}) = \dot{m}_c c_{p,c}(t_{c,i} - t_{c,o}) \tag{2}$$

where $\dot{m}_h$ and $\dot{m}_c$ are the mass-flow rate of the hot and cold fluids, respectively, $c_{p,h}$, and $c_{p,c}$ are the specific heat capacities of the hot and cold fluids, $t_{h.i}$, $t_{c.i}$, $t_{h.o}$, and $t_{c.o}$ are the input and output temperatures of the hot and cold fluids, respectively. The average heat transfer difference between the sides was kept within ±2.5%.

The specific heat capacities, c_p, have been computed based on the experimental data (function of the chemical compound of the crude oil) by:

$$c_p = (0.002t - 1.429)d_{15}^{15} + 0.00267t + 3.049 \tag{3}$$

where t is the temperature and d_{15}^{15} is the relative density at 15°C.

The global heat transfer coefficient, K, can be computed by:

$$Q = KA_e\Delta t_{AM} \tag{4}$$

where A_e is the specific equivalent area of the heat transfer and Δt_{AM} is the arithmetic mean temperature difference, calculated by:

$$\Delta t_{AM} = \frac{1}{2}\left(\frac{t_{h,i} + t_{h,o}}{2} + \frac{t_{c,i} + t_{c,o}}{2}\right) \tag{5}$$

Since we are working in the case of the counter flow of fluids, the logarithmic average was used for the computation of the mean temperature, which is given by:

$$\Delta t_{LMTD}^{cf} = \frac{(t_{h,i} - t_{c,o}) - (t_{h,o} - t_{c,i})}{\ln\dfrac{t_{h,o} - t_{c,i}}{t_{h,i} - t_{c,o}}} \tag{6}$$

Taking into account the flow rate in the tube side, the hydraulic diameter and kinematic viscosity were computed, followed by the estimation of the Reynolds criterion, done by:

$$\mathrm{Re} = \frac{\omega d_\mathrm{h}}{\nu} \tag{7}$$

where ω is the fluid mean velocity, d_h – the hydraulic diameter, and ν – the kinematic viscosity.

The fluid velocity is obtained by.

$$\omega = \frac{4\dot{q}}{\pi d_\mathrm{e}^2} \tag{8}$$

where $\dot{q}$ is the volumetric flow rate, and d_e is the equivalent diameter.

For processing the experimental data and computation of the heat transfer coefficients it is necessary to know as accurately as possible the fluids' characteristics at the working temperature. The physical properties of interest for this study are the densities of the crude oil and gasoline, ρ_co, ρ_g, and the kinematic viscosity of the crude oil and gasoline, ν_co, ν_g, [24], that have to be determined from equations characteristics to the product type. Therefore, the following qualitative indicators have been computed: the absolute density and the kinematic viscosity of the two fluids at 15.6 °C and 37.8 °C (100 F), respectively, in conformity with ASTM D5002-18 [25]. Then, the characteristic equations of the density *vs.* temperature and the kinematic viscosity *vs.* temperature for each fluid have been determined. In our case, the resulted fitted relationships between ρ_co, ρ_g, ν_co, ν_g, and temperature are given in:

$$\rho_\mathrm{co} = -0.0006t + 0.8865 \tag{9}$$

$$\nu_\mathrm{co} = 25.538e^{-0.017t} \tag{10}$$

$$\rho_\mathrm{g} = -0.0005t + 0.711 \tag{11}$$

$$\nu_\mathrm{g} = 1.387e^{-0.006t} \tag{12}$$

Using eqs. (9)-(12), the Reynolds numbers and fluids' velocities have been computed by eqs. (7) and (8).

The fluids' characteristics and geometrical parameters of the heat exchanger are the summarized in tab. 1.

Step 2. At this stage, the input data were 32 data sets formed by recorded inlet temperatures and the Reynolds numbers (computed at *Step 1* for both fluids) and the output were the outlet temperatures. For modeling purposes, GRNN and MLP have been employed. They are artificial intelligence methods, widely used for modeling non-linear phenomena because they do not require an a priori specification of a certain type of equation and do not impose restrictions on the distribution of the input data. They are preferred due to their large applicability [23, 26-28]. The ANN are such types of methods, built using a collection of nodes (called neurons), situated on different layers and connected between them. A neuron receives a signal that it processes and transmits to the neurons connected with it. A neuron has a set of synapses, to which a weight is associated, a function that combines the input, and an activation function, with the role of limiting the signal amplitude.

Table 1. Model's parameters

Parameter	Tube (cold fluid)	Shell (hot fluid)
Density at 15.6 °C, $\rho_{15.6}$, [kg/m^3]	875	705
Kinematic viscosity at 37.8 °C, $v_{37.8}$, [mms^{-1}]	13.27	1.35
Volumetric flow rate, $\dot{q}$, $\dot{m}$ [m^{3}s^{-1}]	0.19	0.13
Inlet temperature [°C]	15	150
Outlet temperature [°C]	80	78
Exterior/interior tube diameter: d_o/d_i [mm]	30/25	–
Tube length, L, [m]	6	–
Number of tubes, N_t	680	–
Shell diameter, D_s, [m]	–	1
Pass number	2	1

The GRNN are feedforward networks composed of four layers (input layer, hidden layer, summation layer, and output layer), formed by neurons [29]. Its structure is presented in fig. 1.

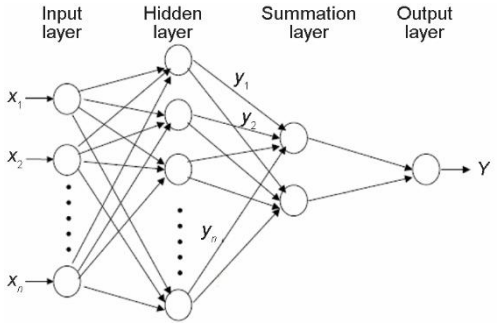

Figure 1. The GRNN structure

The GRNN input layer is formed by one neuron for each predictor variable. The Hidden layer contains a different number of neurons, that can be optimized function of a given criteria. When a vector is introduced in the network, its values are subtracted from those already stored in the vector containing the clusters' centres. The squares or the absolute values of the differences are summed up and introduced into a non-linear activation function – sigmoid, in our case. The summation layer is formed of the numerator and the denominator neurons. The numerator stores the output of addition of the weighted values from the hidden layer. The denominator stores the weighted values from the previous layer multiplied by the corresponding actual target value. The conjugate gradient method is employed to determine the optimal network weights. The output layer is formed by one neuron, that stores the result of the division between the values stored by the neurons from the previous layer [27, 29].

A MLP has an input layer, an output layer and a variable number of hidden layers, fig. 2. The input layer standardizes the input variables values and then distributes them to the neurons in the hidden layer. A bias variable is also introduced, and distributed to the hidden layers, multiplied by a weight and added to the sum going into the neuron [30]. The values coming from the neurons from the input layer are weighted, added up together and introduced into a transfer function in the hidden layer. The results are transferred to the next hidden layer or to the output layer (function of the number of hidden layers). After an analogue weighting procedure, the outputs of the network are produced in the output layer.

In the regression analysis there is a single neuron in the output layer. The activation function of the hidden layer is the logistic function and the activation function for the output layer is the linear one, in this study.

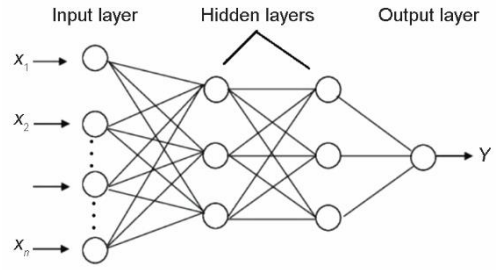

Figure 2. The MLP structure

For estimating the network's parameters, neural networks have to be trained, using the input data. Therefore, the series is divided in two parts, one for training and one for validation. The gradient descent algorithm is used to train the network [30, 31].

The advantages of MLP are the rapidity, and relatively little memory resources necessary, no restrictions related to the data statistical distribution, flexibility and strength of the backpropagation algorithm, ability of increasing the adjustable parameters' number [32].

For the best model selection, the proportion of variance explained by the model, R^2, the correlation between the actual and predicted values, the root mean squared error (RMSE), the mean absolute error (MAE), and the mean absolute percentage error (MAPE) are used. The best model is that for which the indexes have the lowest values. The measurement unit for RMSE, and MAE are the same as those of the variable in the model. The MAPE is a dimensionless parameter, measuring the average of the absolute values of the ratio between the modeling errors and the registered data. They are defined in:

$$\mathrm{MAE}=\frac{1}{n}\sum_{t=1}^{n}\left|y_t-y_t^*\right|,\quad \mathrm{RMSE}=\sqrt{\frac{1}{n}\sum_{t=1}^{n}(y_t-y_t^*)^2},\quad \mathrm{MAPE}=\frac{1}{n}\sum_{t=1}^{n}\left|\frac{y_t-y_t^*}{y_t}\right| \tag{13}$$

where y_t, y_t^* are the actual and computed values, respectively, and n is the sample volume.

It was chosen to compare the results obtained using GRNN against those obtained with MLP because, on one hand, GRNN is faster than MLP and often more accurate and relatively insensitive to outliers and, on the other hand, a two layer backpropagation network with sufficient hidden nodes has been proven to be a universal approximator [33].

Data was divided in two parts, one for training and one for validation, with different ratio between the number of values used for training and validation (70:30, 80:20, and 90:10) for both algorithms. Also, the leave-one-out cross validation has been employed. This approach leaves one data point out of training data, *i.e.* if there are n data points in the original sample then, n-1 samples are used to train the model and one point is used as the validation set. This is repeated for all combinations in which the original sample can be separated this way, and then the error is averaged for all trials, to give overall effectiveness.

For MLP, a single layer and two layers networks were considered and the optimal number of neurons has been selected.

Comparisons of the results are provided. The DTREG software [34] was used for modeling.

Results and discussions

Tables 2-4 contain the results of the models' output estimation in different scenarios. The results from tab. 2 have been obtained by using the smallest error as optimization, for different ratio training: validation (70:30, 80:20, and 90:10) and leave-one-out. The number of neurons in the hidden layer used for modeling, after removing the unused neurons from the network, was 18. While for the training sets, the values of the indexes are the same (up to the forth decimal), for the validation, they are different, the worst ones corresponding to the ratio 90:10, for which the correlation between the actual and predicted values is negative. The best

result has been obtained for the leave-one-out cross-validation, for which we remark values of R^2 and correlation between actual and predicted values close to 1.

Table 3 presents the results of the GRNN output estimation when the optimization criterion was the least number of neurons in the hidden layer. The minimum number of neurons in the hidden layer was determined to be 9 and the best model is that one obtained by leave-one-out validation. It it a little bit worse than leave-one-out when the minimization criterion was the smallest error (tab. 2, last column), but it is still very good (the values of the indicators in both models are quite close).

Table 2. Output from GRNN for different ratio training: validation and the smallest error as optimization criterion

Index	Set	70:30	80:20	90:10	Leave one out
R^2 [%]	Training	95.806	95.805	95.805	95.805
	Validation	85.108	79.123	0.000	90.804
MAE	Training	0.7229	0.7229	0.7229	0.7229
	Validation	1.6846	3.2265	29.6978	1.1464
RMSE	Training	1.0502	1.0502	1.0502	1.0502
	Validation	2.2982	3.1154	46.0673	1.5550
MAPE	Training	1.1182	1.1182	1.1182	1.1182
	Validation	2.4698	2.2909	38.3702	1.7228
Correlation actual-predicted values	Training	0.9799	0.9799	0.9799	0.9799
	Validation	0.9492	0.9060	–0.9314	0.9607

Table 3. Output from GRNN for different ratio training: validation and the smallest number of neurons in the hidden layer as optimization criterion

Index	Sets	70:30	80:20	90:10	Leave one out
R^2 [%]	Training	92.384	92.384	92.384	92.384
	Validation	0.000	75.473	57.567	88.539
MAE	Training	0.887	0.8872	0.8876	0.8872
	Validation	15.3630	1.3485	4.9709	1.2272
RMSE	Training	1.4151	2.1266	1.4151	1.4151
	Validation	31.7288	3.3768	5.3614	1.7359
MAPE	Training	1.3485	1.3485	1.3485	1.3485
	Validation	22.007	2.9843	7.0045	1.8498
Correlation actual-predicted values	Training	0.9635	0.9635	0.9635	0.9635
	Validation	-0.1907	0.9254	0.9155	0.9446

The performances of the MLP with one hidden layer are given in tab. 4. The number of neurons in the hidden layer was optimized by a 4-fold cross-validation and the data used for training and validation were analogous to those used in the GRNN case. The optimal number of neurons in the hidden layer is 3 for the 70:30, 80:20, and 90:10 ratios models and 2

neurons for leave-one-out model, tab. 4 last row. Comparing the performances of MLP models with one hidden layer, tab. 4, the best one in terms of training is that one with the ratio 70:30, while for the validation, differences are notices. The best R^2 is observed for the model with the ratio 90:10, while the best MAE, RMSE and correlation between the actual and predicted values are observed for the *leave-one-out* experiment.

Table 4. Output from MLP with one hidden layer for different ratio training: validation and the smallest error as optimization criterion

Index	Sets	1 hidden layer			
		70:30	80:20	90:10	Leave one out
R^2 [%]	Training	99.568	98.797	98.977	97.665
	Validation	88.971	92.698	93.804	87.816
MAE	Training	0.2045	0.3347	0.3312	0.5997
	Validation	1.4918	1.6198	1.7943	1.4831
RMSE	Training	0.3088	0.5091	0.4692	0.7834
	Validation	1.9778	1.8425	2.0488	1.7898
MAPE	Training	0.3236	0.5162	0.5134	0.9155
	Validation	2.1927	2.4213	2.7895	2.2166
Correlation actual-predicted values	Training	0.9978	0.9939	0.9949	0.9883
	Validation	0.9621	0.9681	0.9967	0.9379
No of neurons		3	3	3	2

Figure 3 illustrates the residual variance variation with respect to the number of neurons in the hidden layer in GRNN and MLP models when the optimization criterion was the smallest error. One remarks a significant variance variation function of the neurons number, especially for MLP. The residual variance in the GRNN models is smaller compared to that for MLP models, but the one with three neurons in the hidden layer. This confirms the finding from tabs. 2-4.

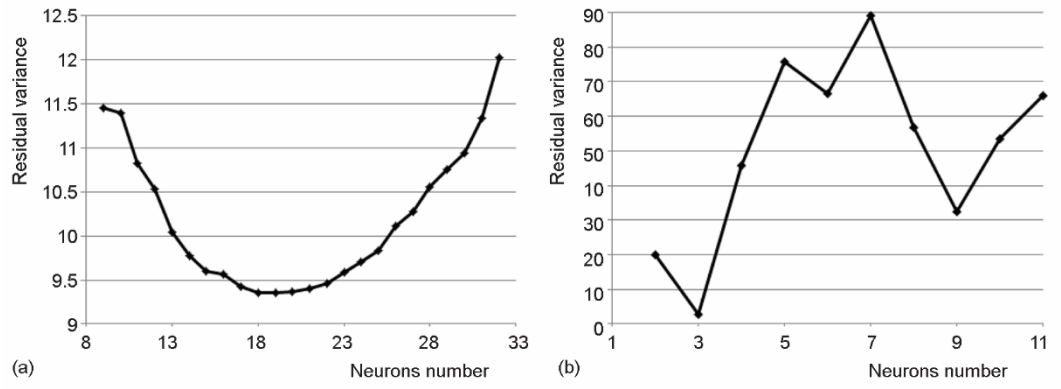

Figure 3. Variance of residual variance function of the number of neurons in the hidden layer for (a) GRNN, (b) MLP with one hidden layer

Table 5 contains the results of the MLP models when the ratio between the training and validation sets is 70:30 with two hidden layers (HL1 and HL2) for different numbers of neurons in the hidden layers. These results are better than those obtained by models with other ratios (not presented in this article for the lack of space). The number of neurons in HL2 was fixed, then the number of neurons in HL1 was optimized. Among these models, that with 2 neurons in HL1 and 5 neurons in HL2 is the best.

Table 5. Output from MLP with two hidden layers (HL1, HL2) for the ratio 70:30 between training: validation and the smallest number of neurons as optimization criterion

Neurons' no		Index	R^2 [%]	MAE	RMSE	MAPE	Correlation actual-predicted values
HL 1	HL2						
2	11	Training	96.114	0.7811	0.8583	1.1673	0.9804
		Validation	87.672	1.6414	2.0910	2.4090	0.9515
2	10	Training	96.61	0.6153	0.8653	0.9139	0.9830
		Validation	84.218	1.7497	2.3658	2.5449	0.9287
7	9	Training	94.994	0.8833	1.0515	1.3407	0.9748
		Validation	92.242	1.5070	1.6588	2.2660	0.9679
4	8	Training	95.414	0.8536	1.0064	1.2867	0.9769
		Validation	94.94	1.2447	1.3397	1.8592	0.9808
3	7	Training	94.994	0.8833	1.1057	1.3407	0.9748
		Validation	88.964	1.6236	1.9784	2.3841	0.9619
6	6	Training	97.992	0.4812	0.6659	0.7322	0.9899
		Validation	88.951	1.5997	1.9795	2.3517	0.9597
2	5	Training	98.315	0.4374	0.6101	0.6750	0.9917
		Validation	96.09	1.0260	1.1776	1.5922	0.9808
4	4	Training	95.985	0.7880	0.9417	1.1802	0.9798
		Validation	90.986	1.4344	1.7880	2.0997	0.9686
5	3	Training	97.099	0.6532	0.8005	0.9806	0.9854
		Validation	89.828	1.5761	1.8994	2.3268	0.9659
2	2	Training	96.329	0.6929	0.9005	1.0290	0.9815
		Validation	85.973	1.7603	2.2305	2.5764	0.9394
4	1	Training	86.142	1.3069	1.7495	1.9800	0.9281
		Validation	91.821	1.3980	1.7032	2.1226	0.9706

Comparing the MLP networks, the model with one hidden layer and ratio 70:30 (tab. 4, column 3) remains the best on the training data set, while the MLP model with 2 neurons in HL1 and 5 neurons in HL2 (tab. 5) is the best on the validation set. The performances of the last model can be visualized on fig. 4, for the training dataset (a) and for the validation one, fig. 4. On these charts, the actual values are plotted against the predicted ones. For a perfect model, the actual and predicted values are equal, so situated on the first diagonal of the chart. fig. 4(b) shows a very good correlation between the actual and predicted values on the train-

ing set and an almost perfect correlation between the actual and predicted values on the validation data. See that in fig. 4(b) the points whose coordinates (measured value, computed value) are situated on the first diagonal of the coordinates axes. This means that the model learned very well the values on the training dataset and applied what it learned on the validation dataset.

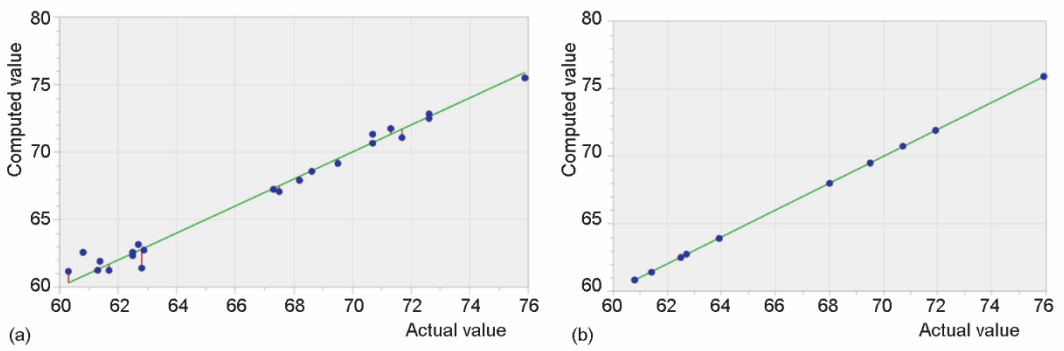

Figure 4. Actual *vs.* predicted values of outlet temperatures on (a) the training data set and (b) the validation data set

Conclusions

In the present study, GRNN and MLP were applied to predict the outlet temperature for heat shell in tube, exchangers using data retrieved from an industrial plant. The network was trained using different percentages of the input data. While for training all the algorithms worked very well, for validation, MLP was superior. It is shown that the best results were obtained using MLP with a ratio of 70:30 for the training and validation sets. The GRNN models give competitive results as well for the ratio 70:30 for the training and validation sets and leave-one-out optimization methods. These results, together with those from the literature mentioned in *Introduction* show that these types of networks can be successfully used in the study of heat transfer in heat exchangers.

For a future work we shall consider the optimization of the heat transfer in different types of heat exchangers, and numerical comparison of different optimization techniques, as in the articles [35-37].

Nomenclature

A – surface area, [m^2]
c_p – specific heat capacity, [Jkg^{-1}K^{-1}]
D_s – shell diameter, [m]
d – tube diameter, [m]
d_h – hydraulic diameter, [m]
d_{15}^{15} – relative density at 15 °C, [–]
K – global heat transfer coefficient, [Wm^{-2}K^{-1}]
L – effective shell length, [m]
$\dot{m}$ – mass-flow rate, [kgs^{-1}]
N_t – number of tubes
$\dot{q}$ – volumetric flow rate, [m^{3}s^{-1}]
Q – termic flux, [W]
Re – Reynolds number, (= $\omega d_h/\nu$), [–]
t – temperature, [°C]
Δt_{LMTD} – logarithmic mean temperature difference, [°C]
Δt_{AM} – arithmetic mean temperature difference, [°C]

Greek symbols

ω – mean velocity, [ms^{-1}]
ρ – density, [kgm^{-3}]
ν – kinematic viscosity, [m^{2}s^{-1}]

Subscripts and superscripts

c – cold
cf – counter flow
co – crude oil

e – equivalent
h – hot
g – gasoline
i – in
o – out

Acronyms

ANN – artificial neural network
GRNN – generalized regression neural network
HL1 – hidden layer 1
HL2 – hidden layer 2
MAE – mean absolute error
MAPE – mean absolute percentage error
MLP – multilayer perception
RMSE – root mean squared error

References

[1] Angsutorn, N., *et al*., Heat Exchanger Network Synthesis Using MINLP Stage-Wise Model with Pinch analysis and Relaxation, *Computer Aided Chemical Engineering, 33* (2014), Jan., pp. 139-144
[2] Barbulescu, A., Dumitriu, C. S., Models of the Mass Loss of Some Copper Alloys, *Chemical Bulletin of Politehnica University (Timisoara)*, *52* (2007), 66, pp. 120-123
[3] Barbulescu, A., Dumitriu, C. S., Mathematical Aspects of the Study of the Cavitation in Liquids, *Proceedings*, 4th Workshop on Mathematical Modeling of Environmental and Sciences Problems, Constanta, Romania, 2006, pp. 7-14
[4] Yeap, B. L., *et al.*, Mitigation of Crude Oil Refinery Heat Exchanger, *Chemical Engineering Research & Design*, *82* (2004), 1, pp. 53-71
[5] Yeap, B. L., *et al.*, Retrofitting Crude Oil Refinery Heat Exchanger Networks to Minimize Fouling While Maximizing Heat Recovery, *Heat Transfer Engineering, 26* (2005), 1, pp. 23-34
[6] Pacheco-Vega, A., *et. al*., On-Line Fuzzy-Logic-Base Temperature Control of a Concentric-Tube Heat Exchanger Facility, *Heat Transfer Engineering*, *30* (2009), 14, pp. 1208-1215
[7] Onishi, V. C., *et. al.*, MINLP Model for the Synthesis of Heat Exchanger Networks with Handling Pressure of Process Streams, *Proceedings*, 24th European Symposium on Computer Aided Process Engineering – ESCAPE, Budapest, Hungary, 2014, pp. 1-6
[8] Xie, G. N., *et .al.*, Heat Transfer Analysis for Shell-and-Tube Heat Exchangers with Experimental Data by Artificial Neural Networks Approach, *Applied Thermal Engineering*, *27* (2007), 5-6, pp. 1096-1104
[9] Parry, A. J., *et al*., Modeling of Thermal Energy Storage Shell-and-Tube Heat Exchanger, *Heat Transfer Engineering*, *35* (2014), 1, pp. 1-14
[10] El-Said, E. M. S., Abou Al-Sood, M. M., Shell and Tube Heat Exchanger With New Segmental Baffles Configurations: A Comparative Experimental Investigation, *Applied Thermal Engineering*, *150* (2019), Mar., pp. 803-810
[11] Guo, Y., *et al.,* Modeling of Plate Heat Exchanger Based on Sensitivity Analysis and Model Updating, *Chemical Engineering Research & Design*, *138* (2018), Oct., pp. 418-432
[12] Li, Q., *et al.,* Compact Heat Exchangers: A Review and Future Applications for a New Generation of high Temperature Solar Receivers, *Renewable and Sustainable Energy Reviews*, *15* (2011), 9, pp. 4855-4875
[13] Shetty, N., *et al.*, Improved Threshold Fouling Models for Crude Oils, *Energy*, *111* (2016), Sept., pp. 453-467
[14] Trzcinski, P., Markowski, M., Diagnosis of the Fouling Effects in a sHell and Tube Heat Exchanger Using Artificial Neural Network, *Chemical Engineering Transactions*, *70* (2018), pp. 355-360
[15] Elankavi S., Shankar, U., Study of Flow and Heat Transfer Analysis in Shell and Tube Heat Exchanger using CFD, *International Research Journal of Engineering and Technology*, *5* (2018), 10, pp. 467-473
[16] Yang, D., *et al*., Geometric Optimization of Shell and Tube Heat Exchanger with Interstitial Twisted Tapes Outside the Tubes Applying CFD Techniques, *Applied Thermal Engineering*, *152* (2019), Apr., pp. 559-572
[17] Abd, A. A., *et al*., Performance Analysis of Shell and Tube Heat Exchanger: Parametric Study, *Case Studies in Thermal Engineering*, *12* (2018), Sept., pp. 563-568
[18] Islamoglu, Y., A New Approach for the Prediction of the Heat Transfer Rate of the Wire-on-Tube Type Heat Exchanger – Use of an Artificial Neural Network Model, *Applied Thermal Engineering*, *23* (2003), 2, pp. 243-249
[19] Moya-Rico, J. D., *et al.*, Characterization of a Triple Concentric-Tube Heat Exchanger with Corrugated Tubes Using Artificial Neural Networks (ANN), *Applied Thermal Engineering*, *147* (2019), Jan., pp. 1036-1046

[20] Pacheco-Vega, A., *et al.*, Neural Network Analysis of Fin-Tube Refrigerating Heat Exchanger with Limited Experimental Data, *International Journal of Heat and Mass Transfer*, *44* (2001), 4, pp. 763-770
[21] Verma, T. N., *et al.*, ANN: Prediction of an Experimental Heat Transfer Analysis of Concentric Tube Heat Exchanger with Corrugated Inner Tubes, *Applied Thermal Engineering*, *120* (2017), June, pp. 219-227
[22] Dheenamma, M., *et al.*, In Pursuit of the Best Artificial Neural Network Configuration for the Prediction of Output Parameters of Corrugated Plate Heat Exchanger, *Fuel*, *239* (2019), Mar., pp. 461-470
[23] Mohanraj, M., *et al.*, Applications of Artificial Neural Networks for Thermal Analysis of Heat Exchangers – A Review, *International Journal of Thermal Sciences*, *90* (2015), Apr., pp. 150-172
[24] Perry, R. J., Green, D. W., *Perry's Chemical Engineers' Handbook*, 7th ed., McGraw-Hill, New York, USA, 1997, pp. 8-28
[25] *** https://www.astm.org/standards/D5002.htm
[26] Dumitriu, C. S., Barbulescu, A., Studies on the Copper-Based Alloys Used in Naval Buildings – Modeling the Mass Loss in Different Media (in Romanian), Sitech, Craiova, Romania, 2007
[27] Barbulescu, A., Barbes, L., Statistical Analysis and Mathematical Models for the VOCs Concentrations on the omanian Littoral, A Case Study, *Analytical Letters, 49* (2016), 3, pp. 387-399
[28] Barbulescu, A., Do the Time Series Statistical Properties Influence the Goodness of Fit of GRNN Models? Study on Financial Series, *Applied Stochastic Models in Business and Industry*, *34* (2018), 5, pp. 586-596
[29] Sprecht, F., A General Regression Neural Network, *IEEE Transactions on Neural Networks*, *2* (1991), 6, pp. 568-576
[30] Rumelhart, D., *et al*., Learning Internal Representations by Error Propagation, in: *Parallel Distributed Processing: Explorations in the Microstructure of Cognition, 1*, MIT Press Cambridge, Cambridge, Mass., USA, 1986, pp. 318-362
[31] Shewchuk, J. R., *An Introduction to the Conjugate Gradient Method Without the Agonizing Pain*, Carnegie Mellon University, Pittsburgh, Penn., USA, 1994, http://www.cs.cmu.edu/~quake-papers/ painless-conjugate-gradient.pdf
[32] Gholami, E., *et al*., Prediction of Viscosity of Several 49 Alumina-Based Nanofluids Using Various Artificial Intelligence Paradigms Comparison with Experimental Data and Empirical Correlations, *Powder Technology*, *323* (2018), Jan., pp. 495-506
[33] Hornik, K., *et al.*, Multilayer Feedforward Networks are Universal Approximators, *Neural Networks*, *2* (1989), 5, pp. 359-366
[34] *** DTREG, https://www.dtreg.com/solution
[35] Grabowska, K., *et al.*, Construction of an Innovative Adsorbent Bed Configuration in the Adsorption Chiller-Selection Criteria for Effective Sorbent-Glue Pair, *Energy*, *151* (2018), May, pp. 317-323
[36] Grabowska, K., *et al.*, The Numerical Comparison of Heat Transfer in a Coated and Fixed Bed of an Adsorption Chiller, *Journal of Thermal Science*, *27* (2018), 5, pp. 421-426
[37] Krzywanski, J., *et al*., An Adaptive Neuro-Fuzzy model of a Re-Heat Two-Stage Adsorption Chiller, *Thermal Science, 23* (2019), Suppl. 4, pp. S1053-S1063

Paper submitted: September 13, 2019
Paper revised: November 5, 2019
Paper accepted: November 7, 2019